A Novel Virus–Host Cell Membrane Interaction: Membrane Voltage–Dependent Endocytic-like Entry of Bacteriophage ϕ6 Nucleocapsid

Minna M. Poranen,*‡ Rimantas Daugelavičius,‡§ Päivi M. Ojala,*‡ Michael W. Hess,* and Dennis H. Bamford*‡

*Institute of Biotechnology and ‡Department of Biosciences, FIN-00014, University of Helsinki, Helsinki, Finland; and §Department of Biochemistry and Biophysics, Vilnius University, LT-2009 Vilnius, Lithuania

Abstract. Studies on the virus–cell interactions have proven valuable in elucidating vital cellular processes. Interestingly, certain virus–host membrane interactions found in eukaryotic systems seem also to operate in prokaryotes (Bamford, D.H., M. Romantschuk, and P.J. Somerharju, 1987. *EMBO (Eur. Mol. Biol. Organ.) J.* 6:1467–1473; Romantschuk, M., V.M. Olkkonen, and D.H. Bamford. 1988. *EMBO (Eur. Mol. Biol. Organ.) J.* 7:1821–1829). ϕ6 is an enveloped double-stranded RNA virus infecting a gram-negative bacterium. The viral entry is initiated by fusion between the virus membrane and host outer membrane, followed by delivery of the viral nucleocapsid (RNA polymerase complex covered with a protein shell) into the host cytosol via an endocytic-like route. In this study, we analyze the interaction of the nucleocapsid with the host plasma membrane and demonstrate a novel approach for dissecting the early events of the nucleocapsid entry process. The initial binding of the nucleocapsid to the plasma membrane is independent of membrane voltage ($\Delta\Psi$) and the K^+ and H^+ gradients. However, the following internalization is dependent on plasma membrane voltage ($\Delta\Psi$), but does not require a high ATP level or K^+ and H^+ gradients. Moreover, the nucleocapsid shell protein, P8, is the viral component mediating the membrane–nucleocapsid interaction.

Key words: endocytosis • cell energetics • dsRNA virus entry • prokaryote • phi6

THE delivery of the viral nucleic acid into the host cell is a complex series of tightly regulated events, where the entering virus utilizes the host cell's machineries to reach its goal. Depending on the host cell and the virus type, different mechanisms have evolved. Classical bacterial virus work demonstrated that the viral DNA is delivered through the host cell envelope leaving the virus capsid outside, whereas animal viruses, in most cases, seem to internalize the viral particle or its subassemblies. Enveloped animal viruses gain access to the host cytosol using membrane fusion. The fusion reaction occurs either at the plasma membrane (PM),[1] as exemplified by members of the families *Paramyxoviridae* and *Retroviridae*, or intracellularly upon endocytic uptake, as with viruses of the families *Togaviridae* and *Orthomyxoviridae*. Nonenveloped animal viruses, such as members of the families *Picornaviridae* and *Adenoviridae*, also mostly rely on endocytosis (Marsh and Helenius, 1989).

The best understood pathway for animal virus internalization occurs via receptor-mediated endocytosis involving coated vesicles and endosomes (Marsh and Helenius, 1989). However, alternative pathways seem to exit. It was recently shown that poliovirus entry is not dependent on the clathrin pathway (DeTulleo and Kirchhausen, 1998). Moreover, morphological studies of polyoma virus, canine parvovirus, and simian virus 40 (SV40) infections have indicated that these nonenveloped viruses can enter via uncoated vesicles (Mackay and Consigli, 1976; Kartenbeck et al., 1989; Basak and Turner, 1992), and recently the SV40 entry was connected to the caveolae pathway (Stang et al., 1997). In the case of SV40 and polyoma viruses, ves-

Address correspondence to Dennis H. Bamford, Viikki Biocenter, P.O. Box 56 (Viikinkaari 5), FIN-00014, University of Helsinki, Finland. Tel.: 358-9-191 59100. Fax: 358-9-191 59098. E-mail: gen_phag@cc.helsinki.fi

P.M. Ojala's present address is Cell Cycle Laboratory, Haartman Institute, University of Helsinki, Finland.

1. *Abbreviations used in this paper*: $\Delta\Psi$, membrane voltage; Δp, proton motive force; ΔpH, transmembrane pH gradient; AP, apyrase; CCCP, carbonyl cyanide m-chlorophenyl hydrazone; CF, chemical fixation; ds, double-stranded; DCCD, *N*,*N*′-dicyclohexylcarbodiimide; FCCP, carbonyl cyanide p-(trifluoromethoxy)phenylhydrazone; FS, freeze substitution; GD, gramicidin D; IC, infective center; MN, monensin; NC, nucleocapsid; NG, nigericin; OM, outer membrane; p.i., postinfection; PM, plasma membrane; PMB, polymyxin B; RF, rapid freezing; TPP^+, tetraphenylphosphonium.

icles appear to be small and tight fitting, in contrast to the uptake via coated vesicles, where the entering virus can be accompanied by detectable amounts of fluid (Marsh and Helenius, 1980).

The endocytic uptake, via coated vesicle, relays on specific proteins that are activated upon ATP or GTP binding or hydrolysis. Both the recycling of the clathrin coat and the dynamin-directed pinching of the coated vesicle from the PM are ATP/GTP-dependent processes (Gao et al., 1991; Hinshaw and Schmid, 1995). The acidic milieu in endosomes is required for the translocation of the viral particle through the membrane of an endocytic vesicle (Marsh and Helenius, 1989). However, it has also been proposed (Carrasco, 1994, 1995) that the proton motive force (Δp), rather than acidic milieu per se, drives this process.

Pseudomonas syringae enveloped bacteriophage ϕ6 is a unique virus in the prokaryotic world. It has a segmented double-stranded (ds) RNA genome (Semancik et al., 1973; Van Etten et al., 1974) and also many other structural and functional characteristics similar to the *Reoviridae.* As the host cells do not possess enzymes to replicate dsRNA, ϕ6, like other dsRNA viruses, has to deliver not only its genome, but also the viral polymerase particle (nucleocapsid core) into the cell to carry out the viral replication cycle. The polymerase complex is the innermost layer in the virion (see Fig. 1, top) and it is composed of four protein species: a particle forming protein (P1) (Ktistakis and Lang, 1987; Olkkonen and Bamford, 1987), an RNA-dependent RNA polymerase (P2) (Juuti and Bamford, 1995), a packaging NTPase (P4) (Gottlieb et al., 1992; Paatero et al., 1995), and a packaging factor (P7) (Juuti and Bamford, 1995). A shell of protein P8 covers the polymerase complex (see Fig. 1, top) in the viral nucleocapsid (NC) (Van Etten et al., 1976). The diameter of the NC is 58 nm (Kenney et al., 1992; Butcher et al., 1997) and, in a mature virus, the NC is enclosed by a lipid envelope (Vidaver et al., 1973). The availability of purified viral components and the unique in vitro genome packaging and replication system allow assembly of infectious viral particles. This makes ϕ6 a model system for dsRNA virus genome packaging, replication, assembly, and maturation (Gottlieb et al., 1988, 1990; Olkkonen et al., 1990; Frilander and Bamford, 1995; Frilander et al., 1995; van Dijk et al., 1995; Qiao et al., 1997; Onodera et al., 1998).

The ϕ6 host is a gram-negative bacterium. The viral lipid envelope, protein P8 shell, and the lytic enzyme P5 are required to deliver the viral core across two membranes and a peptidoglycan layer between them. The current view of the entry mechanism of ϕ6 is illustrated in Fig. 1, bottom. If purified NCs are added to host cell spheroplasts (cells with a removed outer membrane [OM] and peptidoglycan layer), they enter the cell by direct interaction with the exposed PM leading to production of mature infectious virus particles (Ojala et al., 1990).

The entry of ϕ6 is dependent on the energetic state of the host cell (Romantschuk et al., 1988). Apparently the host PM, which in bacterial cells is highly energized, plays a critical role in the entry of the NC into the cytosol. Circulation of protons across the PM plays a primary role in bacterial energy transduction. The respiratory chain as well as the H^+-ATPase at the PM mediate an electrogenic transport of H^+ outwards, maintaining a proton motive force (Δp) across the membrane. Membrane voltage ($\Delta\Psi$, the transmembrane difference of electrical potential) is the major component of Δp, the other component being the pH gradient (ΔpH) (Mitchell, 1979). The proton current loop is completed by molecular devices that allow H^+ to return to the cytosol while performing useful work (ATP synthesis, transport of macromolecules, ions and nutrients, and flagellar motion) at the expense of the Δp or its components (Khan and Macnab, 1980; Nicholls and Ferguson, 1992; Skulachev, 1992; Dreiseikelmann, 1994; Palmen et al., 1994).

The ϕ6 entry mechanism is unique among prokaryotes, but resembles the penetration mechanisms used by both enveloped (fusion with the OM) and nonenveloped (PM penetration by NC) animal viruses (see Fig. 1, bottom). Here we describe, using spheroplast infection, an entry system that allows us to study the NC interactions with the PM and to dissect the early events in NC entry into two stages. The nature of the NC–PM interaction is addressed by using specific agents interfering with the host $\Delta\Psi$, ΔpH, proton pumping, or ATP stability. Moreover, we analyze the role of proteins P1, P2, P4, P7, and P8 in the NC entry.

Materials and Methods

Materials

Wild-type ϕ6 and its host *P. syringae* pathovar phaseolicola HB10Y (Vidaver et al., 1973) were used for NC production. Host cell spheroplasts were prepared from a receptorless phage-resistant derivative of HB10Y, MP0.16 (Romantschuk and Bamford, 1985). LB broth was used as the growth medium (Sambrook et al., 1989).

Monensin (MN), nigericin (NG), valinomycin, carbonyl cyanide m-chlorophenyl hydrazone (CCCP), carbonyl cyanide p-(trifluoromethoxy) phenylhydrazone (FCCP), polymyxin B (PMB) sulfate, polymyxin B nonapeptide, benzoic acid, apyrase (AP), *N*-ethylmaleimide, butylated hydroxytoluene (BHT), and Triton X-114 were purchased from Sigma Chemical Co. KCN, *N,N′*-dicyclohexylcarbodiimide (DCCD), NaF, and tetraphenylphosphonium (TPP^+) chloride were products of Fluka Chemie AG. NaN_3 was obtained from Riedel-deHaën AG, Na_2HAsO_4 from Merck Biochemica, and gramicidin D (GD) from Serva.

NC Isolation

For NC production, bacteriophage ϕ6 was grown on HB10Y and purified as described previously (Olkkonen et al., 1991; Ojala et al., 1993; Bamford et al., 1995). ^{14}C-Labeling of the virus proteins was performed as described by Ojala et al. (1990). The virus spike protein P3 and the viral membrane were removed by treatments with butylated hydroxytoluene and Triton X-114, respectively (Bamford et al., 1995). The NC particles in the Triton X-114 water phase were further purified in 5–20% (wt/vol) sucrose gradients in 20 mM Tris, pH 7.4, 150 mM NaCl (Sorvall AH627 rotor; 24,000 rpm, for 55 min, +15°C) and the light-scattering zone containing the NC was collected using a BioComp gradient fractionator. For the experiments where no salt was preferred, NaCl was omitted from the NC purification. EM analysis was carried out with NC particles pelleted through a 20% (wt/vol) sucrose cushion in 20 mM Tris, pH 8.0, 150 mM NaCl (Beckman Ti50 rotor; 40,000 rpm, for 1 h 25 min, +10°C) after Triton X-114 extraction and resuspended in 12% (wt/vol) sucrose, 20 mM Tris, pH 8, 80 mM NaCl. The NC preparations were used either immediately or stored at −80°C. The protein concentrations of the NC preparations were determined by the Bradford (1976) assay using BSA as a standard, and the protein composition was confirmed by SDS-PAGE (Olkkonen and Bamford, 1989).

Preparation of Host Cell Spheroplasts and Spheroplast Infection

The host cell spheroplasts were prepared as previously described (Ojala et al.,

1990), except that a Sorvall GSA rotor (5,000 rpm, for 6 min, +4°C) was used for centrifugation. The NaCl and Tris–sucrose-treated cells were finally resuspended in ice-cold buffer (20 mM Tris, pH 7.4, 3% [wt/vol] lactose, 2% [wt/vol] BSA) to a cell density of $\sim 10^{10}$ cell/ml, and either used fresh or stored at −80°C in 10% glycerol. The washed cells were treated with lysozyme (5 μg/ml final concentration) and the spheroplasts formed were infected with NCs at a multiplicity of ~50. The standard infection mixture contained ~30 mM NaCl derived from the NC preparation. After the desired time of infection (at 23°C), samples were treated either with NC-specific polyclonal antiserum to inactivate the extracellular NCs or with a nonspecific polyclonal antiserum against bacteriophage PRD1. The infected spheroplasts were diluted in ice-cold buffer (20 mM Tris, pH 7.4, 3% [wt/vol] lactose, 2% [wt/vol] BSA) and plated on a lawn of phage-sensitive HB10Y cells on solid LB. Plates were incubated at 23°C overnight and the infective centers (ICs, infected spheroplasts capable of producing infectious progeny viruses and forming plaques) were counted. The production of progeny phages during the incubation in the test tube was studied by assaying infective viruses in the supernatant of the infection mixture after removal of the spheroplasts by centrifugation.

Determination of ΔΨ, ATP Content, and Ion Fluxes

Extracellular concentrations of H^+, K^+, and TPP^+ ions were monitored at 23°C using ion selective electrodes as previously described (Daugelavičius et al., 1997). The H^+ measurements were carried out using spheroplasts resuspended initially in 2% (wt/vol) BSA, 3% (wt/vol) lactose, pH 7.5. Intracellular K^+ and TPP^+ concentrations were evaluated after permeation of the spheroplasts by GD (8 μg/ml) and PMB (300 μg/ml). The ΔΨ values were calculated using the Nernst equation (Nicholls and Ferguson, 1992). The extracellular ATP content was determined by the luciferin-luciferase method using a 1250 Luminometer (Wallac) and the ATP monitoring reagent from Bio-Orbit. For estimation of intracellular ATP concentration, the spheroplasts were permeated by the ATP releasing reagent (Bio-Orbit) before the ATP measurement. The intracellular volume of the spheroplasts used in the calculations was estimated to be 2% of the total suspension volume. (Based on the cell density and size approximations done in a Bürker chamber).

Drug Treatments and Entry Assay

The effects of monovalent salts, ionophores, and energy-depleting agents on NC infection were studied by measuring the formation of plaques using the entry assay and simultaneously assaying the effects of the drugs on ΔΨ and ATP content of the spheroplasts. Spheroplasts were preincubated with drugs for 2 or 6 min at 23°C, and samples were withdrawn for ΔΨ or ATP measurements and for the NC infection assay. In the standard entry assay, a 50-min infection was followed by an additional 10-min or 7.5-min treatment with NC-specific or nonspecific antiserum, respectively.

Transmission Electron Microscopy

For morphological analysis, NC-infected spheroplasts were subjected either to chemical fixation (CF) or to rapid freezing (RF) and freeze substitution (FS). Spheroplasts were infected with a multiplicity of ~200. Infected spheroplasts (spheroplasts in 30 mM sodium phosphate, pH 6, 3% [wt/vol] lactose, 2% [wt/vol] BSA, 100 mM NaCl, and 50% LB broth) were conventionally fixed with 3% (wt/vol) glutaraldehyde (in 50 mM sodium phosphate, pH 6, 3% [wt/vol] lactose, 2% [wt/vol] BSA) for 15 min at 23°C, followed by OsO_4 after fixation. Before cryoprocessing (RF and FS), spheroplasts were collected (centrifuge 5415, 8,000 rpm, for 2 min, +4°C; Eppendorf-Netheler-Hinz GmbH) and resuspended in 20 mM potassium phosphate, pH 7.4, 3% (wt/vol) lactose, 8% (wt/vol) sucrose, 10% glycerol, 2% (wt/vol) BSA to a cell density of $\sim 6 \times 10^{10}$ cells/ml. Samples from the infection mixtures were rapidly frozen by slamming onto liquid nitrogen–chilled copper blocks, and then freeze-substituted for 8 h at −90°C. Several substitution protocols were tested: (1) acetone and 1–2% (wt/vol) OsO_4, (2) acetone and 1–2% (wt/vol) OsO_4, followed by en-bloc staining with 0.5% (wt/vol) uranyl acetate (for 1 h, +4°C), (3) acetone and 3% (vol/vol) glutaraldehyde, and (4) methanol and 0.5% (wt/vol) uranyl acetate. All samples were embedded in Epon. Thin sections (40–60 nm) were poststained with aqueous 0.5% (wt/vol) uranyl acetate (for 0–40 min at +20–40°C) and lead citrate (for 5 min at +20°C) and viewed at 60–100 kV with a JEOL 1200EX electron microscope.

Neutralization Assay

The NC neutralization tests were carried out with purified mAbs against φ6 structural proteins P1, P4, P8, and P3, (Olkkonen et al., 1988; Ojala et al., 1994) and with polyclonal antiserum against protein P7 (Juuti and Bamford, 1997). The NC specimen was preincubated with antibodies at 23°C for 15 min. Spheroplasts were infected with the NC–antibody mixture for 50 min to determine the amount of ICs.

Results

Spheroplasts Susceptible to NC Infection Are Energetically Active

Earlier studies with intact host cells have indicated that NC penetration through the host PM is an energy-dependent process (Romantschuk et al., 1988). To further analyze the form of energy driving the internalization of the NC, we characterized the energetic state of the uninfected *P. syringae* spheroplasts. A lipophilic cation TPP^+ was used to estimate the ΔΨ values. The distribution of this ion between cells (or organelles) and the surrounding medium can be measured by selective electrodes that monitor the change of the TPP^+ concentration in the incubation medium (Kamo et al., 1979; Grinius et al., 1981). Release of accumulated TPP^+ and cytosolic K^+ ions after addition of a polycationic membrane–active antibiotic PMB or the channel-forming antibiotic GD showed that the PM of the spheroplasts was able to sustain considerable ion gradients. Typically the ΔΨ of intact spheroplasts was between 120 and 150 mV, and the cytosolic K^+ level was ~40 mM. The acidification rate of the spheroplast media was $\sim 2 \times 10^3$ $H^+ \times$ spheroplast$^{-1} \times s^{-1}$, indicating that the proton pumps were actively extruding H^+ ions through the PM. Furthermore, the intracellular ATP level of the spheroplasts was ~600 μM and the extracellular media contained ~3 μM ATP. Although the spheroplasts were rather well energized, their energetic state was not stable when incubated at 23°C with magnetic stirring, the electrochemical measurement conditions (Fig. 2). In these conditions, the spheroplasts became depolarized and the intracellular K^+ leaked out (Fig. 2 b). Simultaneously, the ability of the spheroplasts to support NC infection was dramatically reduced (Fig. 2 a, closed circles). However, storage of spheroplasts on ice without stirring for up to 90 min did not reduce their energetic level or capacity to produce mature viruses (Fig. 2 a, open circles). The instability of the spheroplasts in conditions for electrochemical measurements was taken into account when the effects of different energy-depleting drugs on NC–spheroplast infection were studied. Despite batch-to-batch variation in the ability of the spheroplasts to support NC infection, the trend of the results was consistent and allowed pooling of the data (as in Fig. 5).

During the systematic study of the NC infection, it also became apparent that the maximum virus yield was not affected by the temperature of the infection mixture (10–30°C). However, the rate for achieving the maximum yield was temperature-dependent (not shown). The PM of *P. syringae* cells was permeable to TPP^+ and the cells were sensitive to ionophoric antibiotics GD (a channel former) and NG (a K^+ to H^+ exchanger) even at +6°C, strongly indicating that the PM stays in a fluid state and, thus, is able

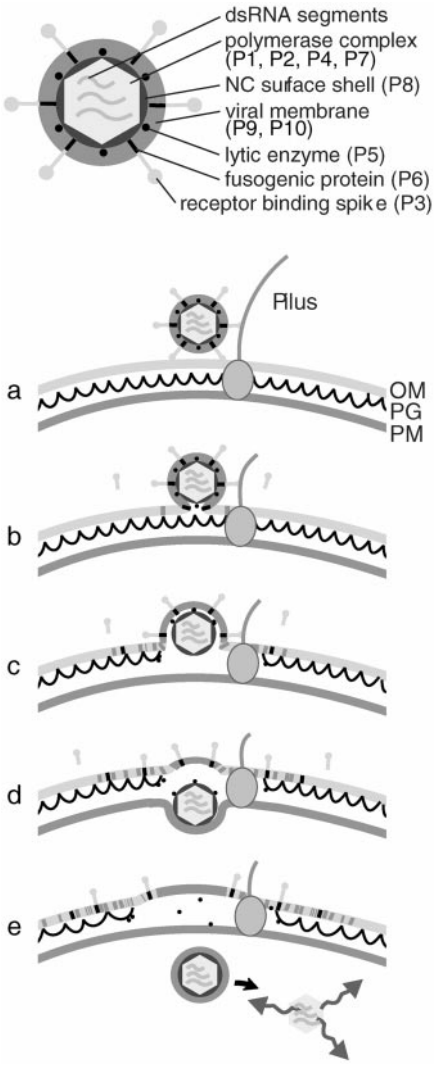

Figure 1. (Top) Schematic presentation of the ϕ6 virion. (Bottom) ϕ6 entry pathway. (a) The infection is initiated by the spike protein P3-mediated adsorption to the pilus receptor (Bamford et al., 1976). (b) Pilus retraction brings the virion into contact with the host's OM (Vidaver et al., 1973; Romantschuk and Bamford, 1985), and the viral envelope undergoes a protein-mediated fusion with the OM (Bamford et al., 1987), placing the viral NC inside the OM. (c) A virus-encoded lytic enzyme P5 on the NC surface locally digests the peptidoglycan (PG) barrier (Mindich and Lehman, 1979; Hantula and Bamford, 1988; Caldentey and Bamford, 1992), which brings the NC into contact with the host's PM. Based on EM data of arrested infections, penetration of the NC particle into the cytosol takes place via a membrane invagination (d) and an intracellular vesicle (e) (Romantschuk et al., 1988) from where the transcriptionally active polymerase particle is released by an unknown mechanism.

to support the formation of invaginations even at low temperatures. Therefore, a low temperature could not be used to dissect the NC binding from the internalization.

The NC Entry Assay

The original NC infection assay (Ojala et al., 1990) was modified to allow the development of an NC entry assay as follows. The comparison of virus progeny production

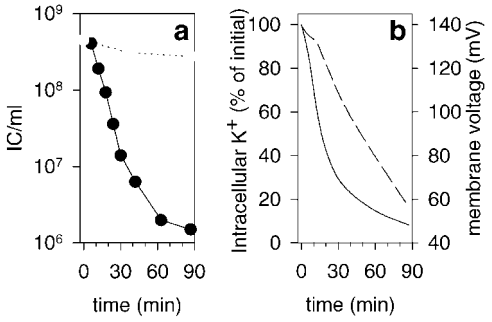

Figure 2. Energetic stability of the *P. syringae* pheroplasts. (a) Spheroplasts at 23°C with magnetic stirring (closed circles) (the conditions of electrochemical measurements) or on ice without stirring (open circles). After different incubation times, samples were taken and infected with NCs. The infection mixtures were diluted and plated out 1 h p.i. to measure the IC formation. (b) Changes in the intracellular K^+ content (solid line) and $\Delta\Psi$ (dashed line) while spheroplasts were incubated with stirring at 23°C.

revealed that both the NC and spheroplasts could be stored frozen without significantly changing the ICs obtained (not shown). This allowed screening of a vast number of conditions using standardized material. The bursting of spheroplasts in the reaction tube at the end of the infection cycle was prevented by the new infection medium containing glycerol but no LB. However, plaques were formed normally when the infected spheroplasts were diluted and plated on a lawn of indicator host on LB plates. Incubation of the infected spheroplasts for up to 4 h at 23°C did not diminish their potential to release infective progeny upon plating.

The time course of IC formation on LB plates after different infection times in a test tube is depicted in Fig. 3 a. The maximal yield is reached at ~45 min postinfection (p.i.). Treatment of the infection mixture with NC-specific polyclonal antiserum allows the dissection of the antibody-inhibitable NC particles (free and PM adsorbed) from those that have already reached an antibody-resistant environment (internalized particles). ICs formed by antibody-resistant NCs as a function of time are shown in Fig. 3 b. In this case, the maximal level is reached at ~90 min. The total yield (Fig. 3 a, closed and open circles) is the sum of the ICs formed by spheroplasts infected both by particles that are adsorbed (antibody inhibitable) and internalized (resistant to the antibody) at the time of plating.

We set up an NC entry assay based on the following three observations: (1) dilution-resistant NCs, inhibitable by antibodies (cell adsorbed particles) can form ICs on plates (Fig. 3 a); (2) a 10-min treatment with NC-specific antiserum causes maximal inactivation of these particles, but still allows the antibody-resistant (internalized) NCs to form ICs (Fig. 3 a, squares); and (3) treatment with the serum did not reduce the ability of spheroplasts to support the viral life cycle (Fig. 3 a, open circles). Thus, in this investigation, NC entry was defined as a process where NCs become resistant to NC-specific antiserum. This was analyzed by comparing the IC counts obtained after a 10-min treatment with an NC-specific antiserum to those obtained after treatment with a nonspecific control antiserum.

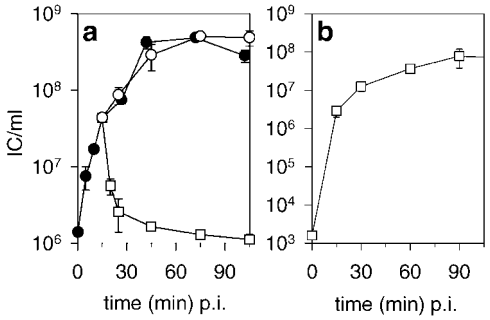

Figure 3. The effects of NC-specific and nonspecific antiserum on IC formation in the NC-spheroplast infection. (a) Formation of IC as a function of time was followed by plating out samples directly from the infection mixture after different incubation times (closed circle). 15 min p.i., samples were withdrawn to antiserum treatments. The effect of the NC-specific (square) and nonspecific (anti-PRD1) (open circle) antiserum was followed by determining the ICs after different incubation times with the serum. (b) Aliquots from NC–spheroplast infection mixture were treated with NC-specific antiserum at 15, 30, 60, and 90 min p.i. and plated out 2 h p.i. The zero point is from an infection where the spheroplasts were infected by NCs pretreated with NC-specific antiserum for 10 min at 23°C.

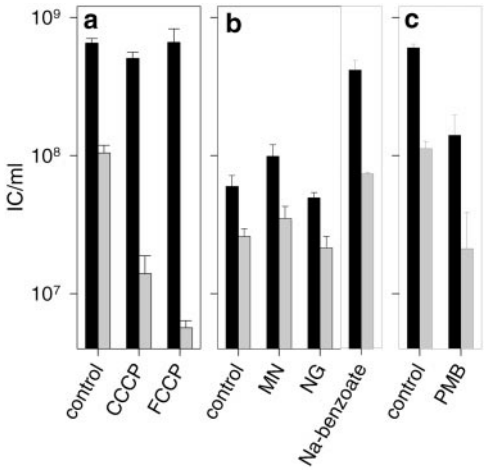

Figure 4. The effect of energy-depleting agents on NC–spheroplasts infection. The NC–spheroplasts infections were carried out in the presence of 25 μg/ml CCCP or FCCP (a), 10 μg/ml MN, 2.5 μg/ml NG or 60 mM Na-benzoate (b), or 200 μg/ml PMB (c). Formation of ICs after treatment with nonspecific (black) or NC-specific (gray) antiserum. (See Materials and Methods for details). The different agents were divided into three categories (a, b, and c) according to their effect on IC formation (see the text). In b (left), the infection mixtures contained no salt leading to lower average IC yields. The effect of sodium benzoate should be compared with the control infections shown in a or c (containing 30 mM NaCl).

The energy requirements of the NC internalization process were analyzed by using energy-depleting agents. Plaque assays, $\Delta\Psi$, and ATP level determinations were simultaneously carried out to monitor the cellular energy status and to correlate it to infection efficiency. As the different agents tested were diluted before plating the infected spheroplasts out, the entered or adsorbed NCs are able to produce progeny on the plates. When a drug inhibits the entry, the number of NCs in the antibody-resistant environment at the time of plating will be lower than in the control infection. However, if the drug does not affect the capability of spheroplasts to produce viruses, or the NC binding to spheroplasts, the antibody-inhibitable NCs (adsorbed to spheroplasts) can enter normally into the spheroplasts after dilution of the drug. Therefore, the number of ICs formed by these NCs will not differ from the control.

NC Internalization Is Dependent on $\Delta\Psi$, but Not on ΔpH

Extensive screening allowed us to find drug concentrations that had measurable effects on the energetic properties of the spheroplasts, but which did not affect IC production per se. On the basis of the effects on the NC entry, the drugs were categorized into three groups as shown in Fig. 4. Compounds in the first category (Fig. 4 a) did not affect the infection per se (Fig. 4 a, black bars), but caused a distinct decrease in plaque numbers if NC-specific antiserum was used, implying an effect on entry (Fig. 4 a, gray bars). This category includes uncouplers of oxidative phosphorylation, CCCP, and FCCP. These protonophores dissipate the Δp (Nicholls and Ferguson, 1992) and, accordingly, reduced $\Delta\Psi$ values (<80 mV) were observed at the concentrations used (25 μg/ml). In spite of the inhibitory effect on entry, the binding of the NC to the spheroplast surface was not reduced because of the decrease in Δp (Fig. 4 a, black bars).

In the second category (Fig. 4 b), the drug treatment had no significant effect on the production of progeny either in the presence or absence of the NC-specific antiserum. MN and NG, the representatives of this category, reduce the existing H^+ and K^+ concentration gradients by exchanging extracellular H^+ for intracellular K^+ ions (Nicholls and Ferguson, 1992). Consistently, an alkalinization of the spheroplast medium and >90% reduction in the cytosolic K^+ content was detected. Moreover, a high concentration of sodium benzoate (a salt of a weak acid) had no effect on NC internalization (Fig. 4 b), thus, further supporting the idea that transmembrane ΔpH is not involved (Nicholls and Ferguson, 1992; Roe et al., 1998).

PMB (a membrane-active antibiotic), *N*-ethylmaleimide (an inhibitor of the SH group–dependent processes), and NaN_3 (an inhibitor of the respiratory chain and membrane H^+-ATP synthase) are examples of drugs falling into the third category (PMB; Fig. 4 c). Active concentrations of these drugs affected the IC formation both in the presence and absence of the NC-specific antiserum. The inhibition of the total IC production (Fig. 4 c, black bars) indicates the following: (1) that incubation with these agents has irreversibly lowered the ability of spheroplasts to produce ICs, (2) the drug is irreversibly bound to membranes and cannot be removed by dilution, or (3) dilution-resistant adsorption of the NCs to spheroplasts has been affected in the presence of the agent. Since the distinction between these alternatives could not be made, these drugs were not used in further studies.

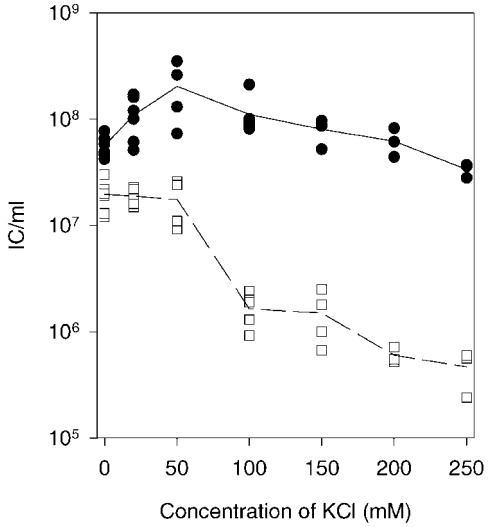

Figure 5. Effect of different K^+ ion concentrations on the IC formation by *P. syringae* spheroplasts. The data points shown are collected from experiments carried out with several different spheroplasts batches. Infections were treated with nonspecific (closed circle) or NC-specific (open square) antiserum.

Increase of the ΔΨ Rescues the NC Internalization

Concentrations of KCl (Fig. 5) or NaCl (not shown) up to 50 mM increased the total yield of ICs. At higher concentrations, reduced ΔΨ values were measured (Fig. 6), and a decrease in the number of ICs after the NC-specific antiserum treatment was detected (Figs. 5 and 6 a). To ensure that the change in the medium osmolarity had not affected the internalization, the osmolarity of the infection mixture was increased with sucrose instead of salt. As shown in Fig. 6 a, the sucrose containing infections did not differ from the control infections.

The inhibitory effect of NaCl and KCl on the NC entry was reversed if MN or NG were added (Fig. 6 a, NG and KCl). However, the electrogenic K^+ carrier, valinomycin, could not rescue the effect of KCl (not shown). The ΔΨ measurements showed that NG also induced an increase in the ΔΨ (Fig. 6 a). Although NG works in an electroneutral manner, it can increase ΔΨ if the respiratory chain is active (Nicholls and Ferguson, 1992). When a portion of KCl was replaced with an inhibitor of the respiratory chain (KCN), the entry effect detected was similar to that in the presence of KCl only (Fig. 6 a). However, NG could not compensate for the reduction in ΔΨ in the presence of KCN nor was the NC entry rescued (Fig. 6 a). Therefore, it appears that there is a threshold value in ΔΨ between 95 and 120 mV (Fig. 6 b) below which the NC internalization is strongly inhibited.

Reduction in Extra- or Intracellular ATP Content Does Not Affect NC Internalization

Different drug treatments were carried out to decrease the intra- and extracellular ATP content of the spheroplasts. To this end, we analyzed the effects of DCCD (an inhibitor of membrane ATP synthase), NaF (an inhibitor of ATP formation from glycolytic substrates), Na_2HAsO_4 (an ATP destabilizing agent), as well as AP (an ATP hydrolyzing enzyme). Some decrease in the ATP concentration was observed in the presence of these agents, but the most efficient reduction was achieved if the spheroplasts were washed before the drug treatments (Fig. 7). The lowest extracellular ATP concentration measured was 75 nM (2.5% of the ATP level of unwashed spheroplasts) and the lowest intracellular ATP concentration was ~50 μM (8% of the ATP level of unwashed spheroplasts). Although some decrease in the total IC production was observed after these treatments, the infections treated with NC-specific antiserum remained at the control level, indicating that internalization of the NC was not affected at reduced ATP concentrations.

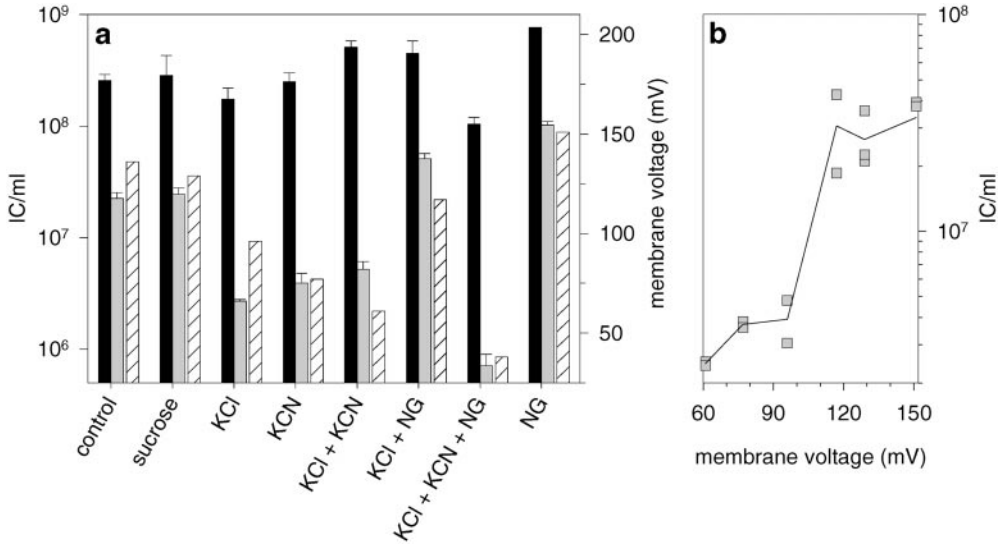

Figure 6. Correlation between membrane voltage and the formation of ICs. Spheroplasts were incubated in the presence of 250 mM sucrose; 125 mM KCl; 25 mM KCN; 85 mM KCl, and 40 mM KCN; 125 mM KCl and 2.0 μg/ml NG; 85 mM KCl, 40 mM KCN and 2.0 μg/ml NG; or 2.0 μg/ml NG. Samples were processed simultaneously in the NC entry assay and for ΔΨ measurements. a represents both the ΔΨ values (hatched), and the IC counts obtained after treatments with nonspecific (black) and NC-specific (gray) antiserum. In b, the ΔΨ values are plotted against the corresponding IC counts from infections treated with NC-specific antiserum. The IC values from a were normalized using IC values obtained after treatment with the nonspecific antiserum.

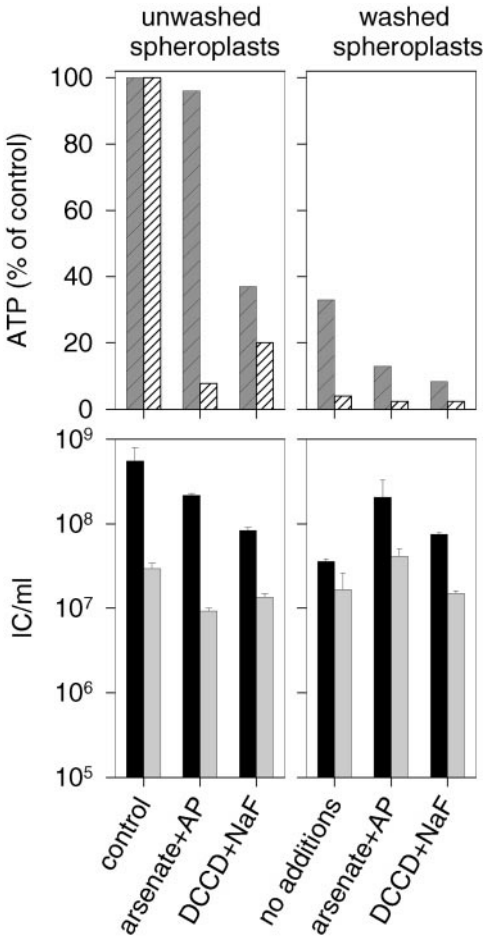

Figure 7. The NC entry assay of spheroplasts with reduced ATP levels. The two top panels show intra- (hatched dark gray) and extracellular (hatched white) ATP content under different conditions. The IC formation from infections carried out under the same conditions is presented in the bottom panels. The infections treated with nonspecific antiserum are shown in black and with NC-specific antiserum in gray. The experiments were carried out with standard spheroplasts used in this study (left) or with spheroplasts that were washed with buffer twice (right). The spheroplasts were incubated in the presence of either 60 mM Na_2HAsO_4 (arsenate) and 20 μg/ml AP, or 20 μM DCCD and 40 mM NaF.

Low pH at the Outer Surface of the PM Is Not Needed for Initial NC Adsorption or Internalization

A high concentration of H^+ ions seems to be crucial for a number of virus entry processes (Marsh and Helenius, 1989; Gaudin et al., 1995). An increase in the pH of the NC infection medium up to 7.5 did not affect the NC internalization (not shown). However, the pH at the outer surface of a metabolically active bacterium can be considerably lower than in the bulk phase of the medium (Koch, 1986). The inhibition of respiration by KCN reduced NC internalization, but it also had a profound effect on $\Delta\Psi$ as shown in Fig. 6 a. The addition of 25 mM KCl or NaCl to the spheroplast suspension caused a clear pulse of acidification of the medium, indicating an exchange of H^+ to K^+ or Na^+ ions at the outer surface of the spheroplasts (not shown). However, this did not considerably affect the IC formation (for KCl see Fig. 5). Neither did the decrease in the surface charge after addition of high concentrations of the polycationic compound, PMB nonapeptide (300 μg/ml), reduce the IC counts (not shown). The density of H^+ at the outer surface of the PM should also be reduced in the presence of NG, which changes the extracellular H^+ to cytosolic K^+, but no inhibition of NC internalization was detected (Fig. 6 a). These results indicate that low pH at the outer surface of the PM is not crucial for the early stages in NC internalization.

EM Reveals NCs at Different Stages of Penetration into the Spheroplast

In a normal ϕ6 infection, practically every cell is infected and the specific infectivity of the virus particles is close to one (Olkkonen and Bamford, 1989). In the NC–spheroplast infection, NCs enter the cells that lack a specific high affinity receptor and high multiplicity of infection is required. In these conditions, approximately every fifth cell is productively infected (Ojala et al., 1990).

Previous morphological analyses of normal ϕ6 infections using freeze-fracture EM showed enveloped NC sized particles in the cell interior in early infection (Bamford and Lounatmaa, 1978). Furthermore, thin section EM analysis of arrested infections has depicted viral NCs entering the cell via a process involving a PM invagination and an intracellular vesicle (Romantschuk et al., 1988). These previous morphological observations suggested an NC–PM interaction mechanism similar to that of eukaryotic endocytosis.

The NC–spheroplast infection system was used to further characterize the NC–PM interactions. As a complement to conventional chemical fixation (CF) (Fig. 8, c and j–m), which may induce artefactual membrane configurations (mesosomes; see Dubochet et al., 1983), we also used RF and FS (Fig. 8, a, b, and d–i). To optimize the FS for this type of material, several different conditions were applied (see Material and Methods). Adequate preservation of bacteria and NC was achieved with OsO_4 in the substitution media Materials and Methods: transmission electron microscopy protocols (1) and (2), which is consistent with the literature (Graham and Beveridge, 1990). However, the triple-layered patterns of the PM were not always seen using this method, a common phenomenon in cryoprocessed bacteria (Dubochet et al., 1983; Graham and Beveridge, 1990). Likewise, in both chemically fixed and cryoprocessed samples, the PM bilayer surrounding the entering viral NCs was not clearly distinguishable from the proteinaceous NC surface shell. However, intracellular enveloped NC particles can be readily distinguished from nonenveloped ones when chemically fixed cells infected with virus mutants producing particles of different composition are analyzed (Bamford and Mindich, 1980). The envelope appears as an ~12-nm-thick diffuse halo surrounding the NC (Fig. 8, i and m). The diffusiveness could be due to the size and density of the particle and the section thickness (Bamford et al., 1976; Bamford and Mindich, 1980). The tight membrane envelope around NC in the virion is visible only when purified virus is embedded in thin layers of vitreous water (Kenney et al., 1992).

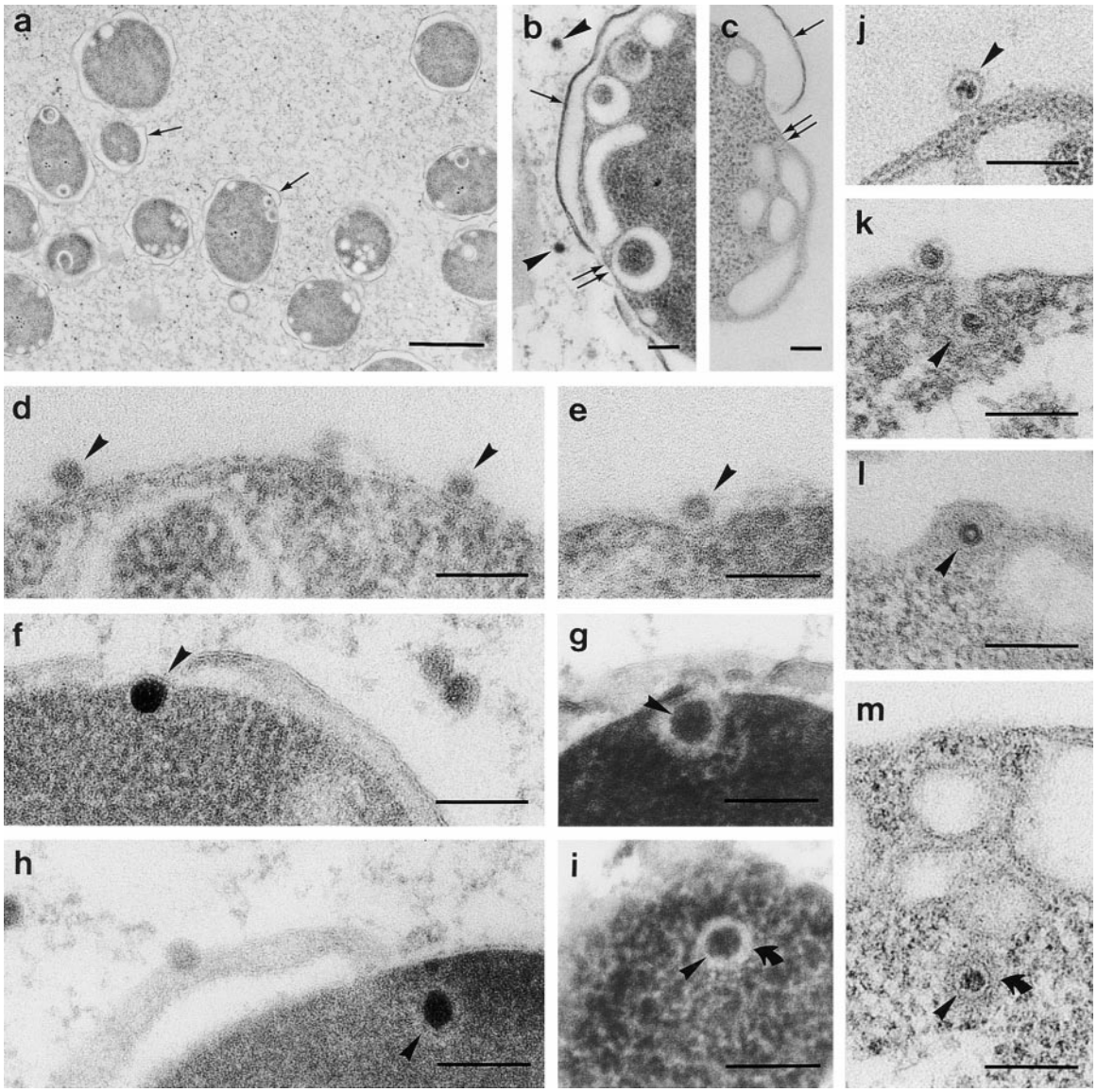

Figure 8. Electron micrographs of *P. syringae* spheroplasts infected with NC for 5–30 min. The bars represent 100 nm, except for a, where the bar represents 1 mm. Arrowheads mark NCs, single arrows mark the OM, and double arrows mark the PM. (a–c) PM invaginations/intracellular vesicles in cryofixed (a and b) and in ambient-temperature chemically fixed (c) spheroplasts (a, control; b, CCCP-treated; and c, NaCl-treated). (d–m) Initial steps in the NC–spheroplast infection: NCs associated with the PM (d and j), in PM indentations (e), invaginations (g and k), and inside the cell (f, h, i, l, and m); the bent arrows in i and m mark the outer limit of the halo made up of the envelope (d–i, cryofixed; and j–m, ambient-temperature chemically fixed).

We carried out the EM analysis at conditions optimized to trap the transient entry event. The infection was arrested by reducing $\Delta\Psi$ either with CCCP or NaCl. As previously documented (Ojala et al., 1990), the *P. syringae* spheroplast appeared spherical and had fragmented OM in loose contact with the cells (Fig. 8, a–c). Regardless of the fixation method or the $\Delta\Psi$ reduction, the spheroplasts constantly displayed PM invaginations and/or intracellular vesicles, indicating them to be intrinsic for spheroplasts, not artifacts of the fixation method (Fig. 8, a–c). The NC-infected spheroplasts showed NC–PM interaction patterns similar to those observed earlier in energy-depleted normal infections (Romantschuk et al., 1988): NCs associated with the PM (Fig. 8, d and j), in PM indentations and invaginations (Fig. 8, e and g and k, respectively), and inside the cell (Fig. 8, f, h, i, l, and m), presumably within tightly fitting membrane vesicles. In the presence of high $\Delta\Psi$, these transient events were difficult to capture, and indentations or invaginations were rare in all samples.

The NC Surface Protein P8 Mediates the NC Interaction with the PM

We also analyzed the role of different NC proteins in NC internalization. Previous studies have suggested the necessity of the protein P8 shell for the NC infectivity; uncoated NC particles devoid of P8 (the NC cores) were not infectious to host cell spheroplasts (Olkkonen et al., 1991), and

certain P8-specific mAbs (8D1 and 8Q2) had a neutralizing effect on NC infectivity (Ojala et al., 1990). We further studied the role of NC proteins P1, P4, P7, and P8 in NC entry using a neutralization assay. A polyclonal P7-specific antiserum and the P1- and P4-specific mAbs that are known to recognize epitopes on the NC surface without aggregating or disrupting the NC (Ojala et al., 1993, 1994) were chosen for the assay. A mAb, 3O4, against P3 (the viral spike protein) was used as a negative control. Neither the P7-specific polyclonal antiserum nor any of the selected P1- or P4-specific mAbs could inhibit the NC infection, indicating that these proteins are not directly involved in the NC entry.

More detailed investigation using the panel of P8-specific mAbs revealed that most of them had a neutralizing effect on NC infectivity (Table I). The nonneutralizing mAbs, 8J3, 8Q4, and 8Q7, did not precipitate NCs in an immunoprecipitation assay, indicating that their epitopes are not accessible on the NC surface (Table I). To confirm that the inhibitory effect was not due to aggregation or disruption of NC particles, the sedimentation assay of NCs was carried out after treatment with several different P8-specific mAbs (Table I). Although many of the neutralizing antibodies did appear to disrupt the NC particles, four nonaggregating and nondisrupting mAbs (8B1, 8D1, 8K4, and 8L1) still had neutralization activity, thus, confirming P8's role in the NC entry.

Discussion

The endocytotic pathway commonly used by eukaryotic cells to internalize different types of molecules and molecular complexes is not thought to function in prokaryotes. However, phage ϕ6 has to use an exceptional entry mechanism to deliver its polymerase complex particle (NC carrying the dsRNA genome) into the host cytosol without dissipating the $\Delta\Psi$. We have shown morphological evidence here and in our previous studies (Bamford and Lounatmaa, 1978; Romantschuk et al., 1988) that this involves association of the NC with the PM, membrane invagination, and release of an enveloped particle into the cytosol. This process resembles the events observed during endocytosis in eukaryotes.

The aim of the present study was to analyze the energy requirements of the ϕ6 endocytic-like NC internalization. Romantschuk and co-workers (1988) showed that this process is dependent on the energetic state of the membrane. However, more detailed analysis of the energy requirements, during infection of an intact cell, is difficult as the initial association of the virus particle with the OM is also an energy-dependent process (Romantschuk et al., 1988). Therefore, purified NCs and host cell spheroplasts were used. We set up an entry assay that allowed us to dissect the NC–PM interaction into two stages: NC adsorption to PM (dilution-resistant antibody-inhibitable state) and NC internalization (antibody-resistant state).

Specific ATP/GTP-dependent cytosolic proteins are needed to direct the normal (clathrin-dependent) endocytic uptake used by many animal viruses (Marsh and Helenius, 1989; Gao et al., 1991; Hinshaw and Schmid, 1995). The form of energy driving the clathrin-independent entry of poliovirus, the SV40 entry via caveolae, or the entry of polyoma virus and canine parvovirus via uncoated vesicles is not clear. Phagocytosis as well as macropinocytosis are directed by actin and ATP (Carlier, 1989; Riezman et al., 1997). However, ATP-independent vesicle formation can be induced in animal cells by exogenous sphingomyelinase treatment (Zha et al., 1998). The translocation of the ϕ6 NC to an antibody-resistant location was not dependent on high extra- or intracellular ATP levels (Fig. 7). Therefore, it seems likely that there are no ATP-dependent cytosolic or PM-associated proteins involved, neither is the viral NTPase activity required.

Δp is commonly used in gram-negative bacteria to drive the transport of macromolecules into or across the membrane(s) (for reviews see Dreiseikelmann, 1994; Palmen et al., 1994). The translocation of phage T4 genome into the host cytosol depends on phage-induced, Δp-dependent fusion of the OM and PM at the site of phage adsorption (Tarahovsky et al., 1991). The insertion of channel-forming colicins into the bacterial PM occurs through an electrostatic binding to the membrane surface, spontaneous insertion of hydrophobic hairpin into the membrane, and $\Delta\Psi$-driven insertion of amphiphilic helices (Cramer et al., 1995). The dilution-resistant ϕ6 NC binding to the spheroplast membrane was not affected at reduced Δp values (Fig. 4 a). However, the subsequent NC transport to the antibody-resistant location was clearly dependent on $\Delta\Psi$ but not on ΔpH (Figs. 4 and 6).

Simultaneous measurements of $\Delta\Psi$ and plaque formation allowed us to define a threshold value for the NC internalization (Fig. 6, ~110 mV). Accordingly, the Δp-dependent processes mentioned above, the T4 phage DNA entry, and the colicin insertion into PM, occur only when

Table I. Characters of Protein P8-specific mAbs

mAb	Epitope accessibility on NC surface*	NC aggregation/disruption‡	Neutralization§
8B1	ND	0	64
8D1	ND	0	32
8J3	−	ND	−
8K1	ND	A/0	32
8K3	+‖	A/D‖	64
8K4	ND	0	32
8L1	ND	0	64
8Q1	ND	A	128
8Q2	+‖	D‖	64
8Q3	ND	A	64
8Q4	−	0	−
8Q5	ND	A	128
8Q7	−	ND	−

*NC–antibody complexes precipitated with protein A–Sepharose CL4B beads as described by Kenney et al. (1992). +, recognition of the NC; −, no precipitation; and ND, not determined.

‡Sedimentation profiles of NC particles treated with different NC-specific mAbs. For the NC-antibody sedimentation assay, a mixture of unlabelled and ^{14}C-labelled NC particles was incubated with mAbs at 23°C for 1 h. The sedimentation analysis was carried out as described by Kenney et al. (1992), and the radioactivity in the fractions was measured using liquid scintillation counting: 0, no changes in the sedimentation of the NC; A, aggregation of the NC; D, disruption of the NC; and ND, not determined.

§The neutralization tests were performed as described in Materials and Methods. The titer represent the last dilution giving a 60% reduction in the number of ICs. A polyclonal NC-specific antiserum and mAbs against ϕ6 spike protein P3 were used as positive and negative controls, respectively. The titer of the NC-specific antiserum in this assay was 1,600.

‖Ojala et al. (1993).

the $\Delta\Psi$ is above a threshold value (Dreiseikelmann, 1994; Palmen et al., 1994; Cramer et al., 1995). Similarly to the colicin insertion, the $\Delta\Psi$ dependence in NC entry might be associated to polypeptide chain translocation (probably of the NC shell protein P8) into the PM. Alternatively, the $\Delta\Psi$ might be required as the NC-containing invagination pinches off from the PM. In the bacterial PM, the negatively charged phospholipids, cardiolipin and phospatidylglycerol, are predominantly located in the outer leaflet and phosphatidylethanolamine in the inner leaflet (Card and Trautman, 1990). The transport of phosphatidylethanolamine from one leaflet to another is dependent on Δp (Donohue-Rolfe and Schaechter, 1980). The fusion of an NC-containing invagination might require the transport of phosphatidylethanolamine as only this bacterial phospholipid can support membrane fusion (Chernomordik et al., 1995).

The NC surface protein P8 was shown to be crucial for the entry. Viral proteins involved in the entry are known to undergo large conformational changes (see for example Bullough et al., 1994). These changes are triggered by the receptor binding and/or by the low pH during endocytosis. Our preliminary results indicate that acidic conditions change the conformation of P8, suggesting that protonation is also involved in the NC entry process. However, the tight coupling of proton pumping and $\Delta\Psi$ production makes it difficult to dissect these effects (Fig. 6). The NC adsorption and early steps in the formation of the PM invagination were not affected in conditions where the PM surface charge, and thus protonation, was reduced. We consider that the proton-dependent events are crucial later in the entry, in the process of the NC release from the entry vesicle.

ϕ6 entry can now be dissected into a number of stages (Fig. 1, bottom) (Bamford et al., 1976, 1987; Mindich and Lehman, 1979; Romantschuk and Bamford, 1985; Romantschuk et al., 1988; this investigation). The present investigation sheds light on the NC absorption to the PM and subsequent processes. We are actively studying the last step in the infection process, the release of the polymerase complex from the vesicle and its subsequent activation. The accumulated data on the ϕ6 entry process interestingly highlights common universal mechanisms operating in both prokaryotic and eukaryotic cells, and points out that mechanisms that were thought to operate in eukaryotes only are also used in prokaryotes.

Sarah Butcher is acknowledged for critical reading of the manuscript. Marja-Leena Perälä (both from Institute of Biotechnology) is thanked for her skilful technical assistance and Arja Strandell (EM Unit, Institute of Biotechnology) for thin-sections.

This work has been supported by Finnish Academy of Science (grants 30562 and 37725) and EU grant B104-CT97-2364.

Submitted: 21 July 1998
Revised: 16 August 1999
Accepted: 21 September 1999

References

Bamford, D.H., and K. Lounatmaa. 1978. Freeze-fracturing of *Pseudomonas phaseolicola* infected by the lipid-containing bacteriophage ϕ6. *J. Gen. Virol.* 39:161–170.

Bamford, D.H., and L. Mindich. 1980. Electron microscopy of cells infected with nonsense mutants of bacteriophage ϕ6. *Virology*. 107:222–228.

Bamford, D.H., E.T. Palva, and K. Lounatmaa. 1976. Ultrastructure and life cycle of the lipid-containing bacteriophage ϕ6. *J. Gen. Virol*. 32:249–259.

Bamford, D.H., M. Romantschuk, and P.J. Somerharju. 1987. Membrane fusion in prokaryotes: bacteriophage ϕ6 membrane fuses with the *Pseudomonas syringae* outer membrane. *EMBO (Eur. Mol. Biol. Organ.) J.* 6:1467–1473.

Bamford, D.H., P.M. Ojala, M. Frilander, L. Wallin, and J.K.H. Bamford. 1995. Isolation, purification, and function of assembly intermediates and subviral particles of bacteriophage PRD1 and ϕ6. *Methods Mol. Genet.* 6:455–474.

Basak, S., and H. Turner. 1992. Infectious entry pathway for canine parvovirus. *Virology*. 186:368–376.

Bradford, M.M. 1976. A rapid and sensitive method for the quantification of microgram quantities of protein utilizing the principle of protein-dye binding. *Anal. Biochem*. 72:248–254.

Bullough, P.A., F.M. Hughson, J.J. Skehel, and D.C. Wiley. 1994. The structure of the influenza haemagglutinin at the pH of membrane fusion. *Nature*. 371: 37–43.

Butcher, S.J., T. Dokland, P.M. Ojala, D.H. Bamford, and S.D. Fuller. 1997. Intermediates in the assembly pathway of the double-stranded RNA virus ϕ6. *EMBO (Eur. Mol. Biol. Organ.) J.* 16:4477–4487.

Caldentey, J., and D.H. Bamford. 1992. The lytic enzyme of the *Pseudomonas* phage ϕ6. Purification and biochemical characterization. *Biochim. Biophys. Acta*. 1159:44–50.

Card, G.L., and J.K. Trautman. 1990. Role of anionic lipid in bacterial membranes. *Biochim. Biophys. Acta*. 1047:77–82.

Carlier, M.F. 1989. Role of nucleotide hydrolysis in the dynamics of actin filaments and microtubules. *Int. Rev. Cytol*. 115:139–170.

Carrasco, L. 1994. Entry of animal viruses and macromolecules into cells. *FEBS (Fed. Eur. Biochem. Soc.) Lett.* 350:151–154.

Carrasco, L. 1995. Modification of membrane permeability by animal viruses. *Adv. Virus. Res*. 45:61–112.

Chernomordik, L., M.M. Kozlov, and J. Zimmerberg. 1995. Lipids in biological membrane fusion. *J. Memb. Biol*. 146:1–14.

Cramer, W.A., J.B. Heymann, S.L. Schendel, B.N. Deriy, F.S. Cohen, P.A. Elkins, and C.V. Stauffacher. 1995. Structure-function of the channel-forming colicins. *Annu. Rev. Biophys. Biomol. Struct*. 24:611–641.

Daugelavičius, R., J.K. Bamford, and D.H. Bamford. 1997. Changes in host cell energetics in response to bacteriophage PRD1 DNA entry. *J. Bacteriol*. 179: 5203–5210.

DeTulleo, L., and T. Kirchhausen. 1998. The clathrin endocytic pathway in viral infection. *EMBO (Eur. Mol. Biol. Organ.) J.* 17:4585–4593.

Donohue-Rolfe, A.M., and M. Schaechter. 1980. Translocation of phospholipids from the inner to the outer membrane of *Escherichia coli. Proc. Natl. Acad. Sci. USA*. 77:1867–1871.

Dreiseikelmann, B. 1994. Translocation of DNA across bacterial membranes. *Microbiol. Rev*. 58:293–316.

Dubochet, J., A.W. McDowall, B. Menge, E.N. Schmid, and K.G. Lickfeld. 1983. Electron microscopy of frozen-hydrated bacteria. *J. Bacteriol*. 155: 381–390.

Frilander, M., and D.H. Bamford. 1995. In vitro packaging of the single-stranded RNA genomic precursors of the segmented double-stranded RNA bacteriophage ϕ6: the three segments modulate each other's packaging efficiency. *J. Mol. Biol*. 246:418–428.

Frilander, M., M. Poranen, and D.H. Bamford. 1995. The large genome segment of dsRNA bacteriophage ϕ6 is the key regulator in the in vitro minus and plus strand synthesis. *RNA*. 1:510–518.

Gao, B.C., J. Biosca, E.A. Craig, L.E. Greene, and E. Eisenberg. 1991. Uncoating of coated vesicles by yeast hsp70 proteins. *J. Biol. Chem*. 266:19565–19571.

Gaudin, Y., R.W. Ruigrok, and J. Brunner. 1995. Low-pH induced conformational changes in viral fusion proteins: implications for the fusion mechanism. *J. Gen. Virol*. 76:1541–1556.

Gottlieb, P., J. Strassman, D.H. Bamford, and L. Mindich. 1988. Production of a polyhedral particle in *Escherichia coli* from a cDNA copy of the large genomic segment of bacteriophage ϕ6. *J. Virol*. 62:181–187.

Gottlieb, P., J. Strassman, X.Y. Qiao, A. Frucht, and L. Mindich. 1990. In vitro replication, packaging, and transcription of the segmented double-stranded RNA genome of bacteriophage ϕ6: studies with procapsids assembled from plasmid-encoded proteins. *J. Bacteriol*. 172:5774–5782.

Gottlieb, P., J. Strassman, and L. Mindich. 1992. Protein P4 of the bacteriophage ϕ6 procapsid has a nucleoside triphosphate-binding site with associated nucleoside triphosphate phosphohydrolase activity. *J. Virol*. 66:6220–6222.

Graham, L.L., and T.J. Beveridge. 1990. Evaluation of freeze-substitution and conventional embedding protocols for routine electron microscopic processing of eubacteria. *J. Bacteriol*. 172:2141–2149.

Grinius, L., R. Daugelavičius, and G. Alkimavičius. 1981. Studies of the membrane potential of *Bacillus subtilis* and *Escherichia coli* cells by the method of penetrating ions. *Biochemistry (Moscow)*. 45:1222–1230.

Hantula, J., and D.H. Bamford. 1988. Chemical crosslinking of bacteriophage ϕ6 nucleocapsid proteins. *Virology*. 165:482–488.

Hinshaw, J.E., and S.L. Schmid. 1995. Dynamin self-assembles into rings suggesting a mechanism for coated vesicle budding. *Nature*. 374:190–192.

Juuti, J.T., and D.H. Bamford. 1995. RNA binding, packaging and polymerase activities of the different incomplete polymerase complex particles of dsRNA bacteriophage ϕ6. *J. Mol. Biol*. 249:545–554.

Juuti, J.T., and D.H. Bamford. 1997. Protein P7 of phage ϕ6 RNA polymerase

complex, acquiring of RNA packaging activity by in vitro assembly of the purified protein onto deficient particles. *J. Mol. Biol*. 266:891–900.
Kamo, N., M. Muratsugu, R. Hongoh, and Y. Kobatake. 1979. Membrane potential of mitochondria measured with an electrode sensitive to tetraphenyl phosphonium and relationship between proton electrochemical potential and phosphorylation potential in steady state. *J. Memb. Biol*. 49:105–121.
Kartenbeck, J., H. Stukenbrok, and A. Helenius. 1989. Endocytosis of simian virus 40 into the endoplasmic reticulum. *J. Cell. Biol*. 109:2721–2729.
Kenney, J.M., J. Hantula, S.D. Fuller, L. Mindich, P.M. Ojala, and D.H. Bamford. 1992. Bacteriophage ϕ6 envelope elucidated by chemical cross-linking, immunodetection, and cryoelectron microscopy. *Virology*. 190:635–644.
Khan, S., and R.M. Macnab. 1980. The steady-state counterclockwise/clockwise ratio of bacterial flagellar motors is regulated by proton motive force. *J. Mol. Biol*. 138:563–597.
Koch, A.L. 1986. The pH in the neighborhood of membranes generating a protonmotive force. *J. Theor. Biol*. 120:73–84.
Ktistakis, N.T., and D. Lang. 1987. The dodecahedral framework of the bacteriophage ϕ6 nucleocapsid is composed of P1. *J. Virol.* 61:2621–2623.
Mackay, R.L., and R.A. Consigli. 1976. Early events in polyoma virus infection: attachment, penetration, and nuclear entry. *J. Virol*. 19:620–636.
Marsh, M., and A. Helenius. 1980. Adsorptive endocytosis of Semliki forest virus. *J. Mol. Biol.* 142:439–454.
Marsh, M., and A. Helenius. 1989. Virus entry into animal cells. *Adv. Virus Res.* 36:107–151.
Mindich, L., and J. Lehman. 1979. Cell wall lysin as a component of the bacteriophage ϕ6 virion. *J. Virol.* 30:489–496.
Mitchell, P. 1979. The Ninth Sir Hans Krebs Lecture. Compartmentation and communication in living systems. Ligand conduction: a general catalytic principle in chemical, osmotic and chemiosmotic reaction systems. *Eur. J. Biochem*. 95:1–20.
Nicholls, D.G., and J.S. Ferguson. 1992. Bioenergetics 2. Academic Press Inc., London. 255 pp.
Ojala, P.M., M. Romantschuk, and D.H. Bamford. 1990. Purified ϕ6 nucleocapsids are capable of productive infection of host cells with partially disrupted outer membranes. *Virology*. 178:364–372.
Ojala, P.M., J.T. Juuti, and D.H. Bamford. 1993. Protein P4 of double-stranded RNA bacteriophage ϕ6 is accessible on the nucleocapsid surface: epitope mapping and orientation of the protein. *J. Virol*. 67:2879–2886.
Ojala, P.M., A.O. Paatero, and D.H. Bamford. 1994. NTP binding induces conformational changes in the double-stranded RNA bacteriophage ϕ6 subviral particles. *Virology*. 205:170–178.
Olkkonen, V.M., and D.H. Bamford. 1987. The nucleocapsid of the lipid-containing double-stranded RNA bacteriophage ϕ6 contains a protein skeleton consisting of a single polypeptide species. *J. Virol*. 61:2362–2367.
Olkkonen, V.M., and D.H. Bamford. 1989. Quantitation of the adsorption and penetration stages of bacteriophage ϕ6 infection. *Virology*. 171:229–238.
Olkkonen, V.M., P.M. Pekkala, and D.H. Bamford. 1988. Monoclonal antibodies to the major structural proteins of bacteriophage ϕ6. *Virology*. 165:317–320.
Olkkonen, V.M., P. Gottlieb, J. Strassman, X.Y. Qiao, D.H. Bamford, and L. Mindich. 1990. In vitro assembly of infectious nucleocapsids of bacteriophage ϕ6: formation of a recombinant double-stranded RNA virus. *Proc. Natl. Acad. Sci. USA*. 87:9173–9177.
Olkkonen, V.M., P.M. Ojala, and D.H. Bamford. 1991. Generation of infectious nucleocapsids by in vitro assembly of the shell protein on to the polymerase complex of the dsRNA bacteriophage ϕ6. *J. Mol. Biol*. 218:569–581.
Onodera, S., X. Qiao, J. Qiao, and L. Mindich. 1998. Directed changes in the number of double-stranded RNA genomic segments in bacteriophage ϕ6. *Proc. Natl. Acad. Sci. USA*. 95:3920–3924.
Paatero, A.O., J.E. Syvaoja, and D.H. Bamford. 1995. Double-stranded RNA bacteriophage ϕ6 protein P4 is an unspecific nucleoside triphosphatase activated by calcium ions. *J. Virol*. 69:6729–6734.
Palmen, R., A.J. Driessen, and K.J. Hellingwerf. 1994. Bioenergetic aspects of the translocation of macromolecules across bacterial membranes. *Biochim. Biophys. Acta*. 1183:417–451.
Qiao, X., J. Qiao, and L. Mindich. 1997. Stoichiometric packaging of the three genomic segments of double-stranded RNA bacteriophage ϕ6. *Proc. Natl. Acad. Sci. USA*. 94:4074–4079.
Riezman, H., P.G. Woodman, G. van Meer, and M. Marsh. 1997. Molecular mechanisms of endocytosis. *Cell*. 91:731–738.
Roe, A.J., D. McLaggan, I. Davidson, C. O'Byrne, and I.R. Booth. 1998. Perturbation of anion balance during inhibition of growth of *Escherichia coli* by weak acids. *J. Bacteriol*. 180:767–772.
Romantschuk, M., and D.H. Bamford. 1985. Function of pili in bacteriophage ϕ6 penetration. *J. Gen. Virol*. 66:2461–2469.
Romantschuk, M., V.M. Olkkonen, and D.H. Bamford. 1988. The nucleocapsid of bacteriophage ϕ6 penetrates the host cytoplasmic membrane. *EMBO (Eur. Mol. Biol. Organ.) J.* 7:1821–1829.
Sambrook, J., E.F. Fritsch, and T. Maniatis. 1989. Molecular Cloning: A Laboratory Manual. Cold Spring Harbor Laboratory, Cold Spring Harbor, New York.
Semancik, J.S., A.K. Vidaver, and J.L. Van Etten. 1973. Characterization of segmented double-helical RNA from bacteriophage ϕ6. *J. Mol. Biol.* 78: 617–625.
Skulachev, V.P. 1992. The laws of cell energetics. *Eur. J. Biochem*. 208:203–209.
Stang, E., J. Kartenbeck, and R.G. Parton. 1997. Major histocompatibility complex class I molecules mediate association of SV40 with caveolae. *Mol. Biol. Cell*. 8:47–57.
Tarahovsky, Y.S., A.A. Khusainov, A.A. Deev, and Y.V. Kim. 1991. Membrane fusion during infection of *Escherichia coli* cells by phage T4. *FEBS (Fed. Eur. Biochem. Soc.) Lett.* 289:18–22.
van Dijk, A.A., M. Frilander, and D.H. Bamford. 1995. Differentiation between minus- and plus-strand synthesis: polymerase activity of dsRNA bacteriophage ϕ6 in an in vitro packaging and replication system. *Virology*. 211: 320–323.
Van Etten, J.L., A.K. Vidaver, R.K. Koski, and J.P. Burnett. 1974. Base composition and hybridization studies of the three double-stranded RNA segments of bacteriophage ϕ6. *J. Virol.* 13:1254–1262.
Van Etten, J.L., L. Lane, C. Gonzales, J. Partridge, and A. Vidaver. 1976. Comparative properties of bacteriophage ϕ6 and ϕ6 nucleocapsid. *J. Virol.* 18: 652–658.
Vidaver, A.K., R.K. Koski, and J.L. Van Etten. 1973. Bacteriophage ϕ6: a lipid-containing virus of *Pseudomonas phaseolicola*. *J. Virol.* 11:799–805.
Zha, X., L.M. Pierini, P.L. Leopold, P.J. Skiba, I. Tabas, and F.R. Maxfield. 1998. Sphingomyelinase treatment induces ATP-independent endocytosis. *J. Cell. Biol*. 140:39–47.